

Materials Horizons

Accepted Manuscript



This is an *Accepted Manuscript*, which has been through the Royal Society of Chemistry peer review process and has been accepted for publication.

Accepted Manuscripts are published online shortly after acceptance, before technical editing, formatting and proof reading. Using this free service, authors can make their results available to the community, in citable form, before we publish the edited article. We will replace this *Accepted Manuscript* with the edited and formatted *Advance Article* as soon as it is available.

You can find more information about *Accepted Manuscripts* in the [Information for Authors](#).

Please note that technical editing may introduce minor changes to the text and/or graphics, which may alter content. The journal's standard [Terms & Conditions](#) and the [Ethical guidelines](#) still apply. In no event shall the Royal Society of Chemistry be held responsible for any errors or omissions in this *Accepted Manuscript* or any consequences arising from the use of any information it contains.

Cite this: DOI: 10.1039/c0xx00000x

www.rsc.org/xxxxxx

ARTICLE TYPE

Nanoarray based “Superaerophobic” Surfaces for Gas Evolution Reaction Electrodes

Zhiyi Lu,^{†a} Yingjie Li,^{†a} Xiaodong Lei,^a Junfeng Liu^a and Xiaoming Sun^{*a}

Received (in XXX, XXX) Xth XXXXXXXXX 20XX, Accepted Xth XXXXXXXXX 20XX

DOI: 10.1039/b000000x

Electrochemical gas evolution reactions are now of great importance in energy conversion processes and industries, and the keys for improving the catalytic performances lie in developing efficient catalytic electrodes. Besides the exploration of highly active catalysts, fast removal of the gas products on the electrode surface should be realized because the adhered gas bubbles would block the following catalytic reactions and decrease the efficiency. In this paper, we introduced an ideal structure, “superaerophobic” surface, to diminish the negative effects caused by the adhered gas bubbles. Several recent works focusing on addressing this issue are presented with the target reactions of hydrogen evolution and oxygen evolution. It is demonstrated that micro/nano-engineering of the catalyst directly on the current collector is a promising approach to minimize the negative effective induced by the gas bubble adhesion. At the last section, we have also discussed the promise of this methodology for other energy related systems.

1. Introduction

Gas evolution reactions (GERs), which are processes of converting liquid reactants to gas products accompanied with electrons transfer in aqueous mediums, are of great importance in various industries, covering a number of energy storage and conversion systems. Hydrogen evolution reaction (HER) and oxygen evolution reaction (OER) are two essential components for electrochemical water splitting, which is considered as one of the most effective approach for future energy solution.^{1, 2} In addition, OER is also crucial in the charge process for rechargeable metal-air batteries^{3, 4}, and HER is necessary for chlor-alkali industry⁵ as well as chlorine evolution reaction (CIER). GERs also hold keys in anodic reactions in direct liquid fuel cells, such as methanol oxidation and hydrazine oxidation.⁶⁻⁸

For the above mentioned GERs, catalysts are required to reduce the overpotentials for achieving high reaction rates (i.e. high current densities). Constructing ideal catalytic electrodes for GERs should follow three principles. Firstly, for each target reaction, the catalyst selected should possess a high intrinsic activity, which is determined by the electronic structure of the active center.⁹⁻¹⁶ Secondly, the catalyst film should be porous and with high electric conductivity, which permits the penetration of the electrolyte and accelerates the electron transfer throughout the whole electrode.¹⁷⁻¹⁹ Thirdly, the surface of the catalytic electrode should be easy to release the as-formed gas bubble product because severe adhesion of the gas bubble will block the contact between the catalyst and reactant, cause excessive ohmic drop and thereby decrease the efficiency.²⁰ Although it is reported that inducing ultragravity²¹ or ultrasonic treatment²² is beneficial to the disengagement process of gas bubbles, however, they are not cost-effective for industrial production.

This review summarized several recent works focusing on nanoscale electrode surface engineering to address the third

principle of constructing an efficient catalytic electrode, which simultaneously meets the first and second principles. It is demonstrated that micro/nano-engineering of the catalyst directly on the current collector to gain a low-adhesion electrode is a promising approach to minimize the negative effective induced by the gas bubble adhesion. A new concept, “superaerophobic” surface, is introduced to describe the interaction between gas bubbles and the low-adhesion electrodes. HER and OER are the target reactions shown here, and the optimized architectures for the various catalysts are presented. At the last section, the promise of this methodology for GERs in other systems is also discussed.

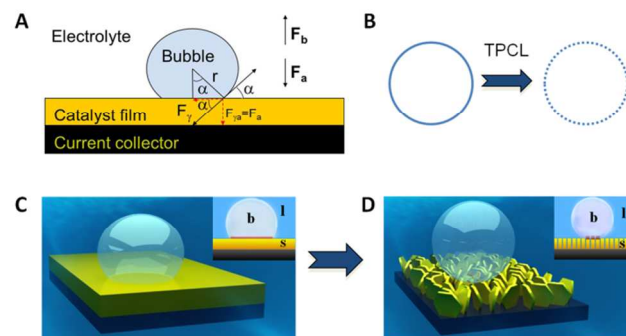


Figure 1. (A), force analysis of a single gas bubble sitting on the catalyst film; (B), triple-phase contact lines (TPCLs) on the flat film (left) and nanostructured film (right); (C) and (D), schematic illustration of the adhesion behaviors of gas bubbles on flat film (left) and nanostructured film (right). Inset: side views to show the different intact and discontinuous TPCL on flat and nanostructured films, also the different contact angles. The brown zone is “dead area” isolated by as-formed bubble. (Reprinted with permission from Ref. [20], Copyright 2014, Wiley-VCH)

2. Mechanism to design low-adhesion electrodes

As the reactant is liquid and the product is gas in GERs, a three-phase interface is formed together with the solid electrode, as shown in Figure 1A. If the as-formed gas bubbles melt and form a gas film, the electrolyte diffusion to the electrode surface will be blocked. Accordingly, the electrode surface should be able to readily release gas products. Thus, how to make the surface dislike the gas product is the main challenge in constructing the architecture of the catalyst film. For a single gas bubble sitting on the surface of catalyst film (Figure 1A), it suffers two main forces: one is the buoyant force (F_b) that is proportional to the volume of the gas bubble assuming that the shape of the gas bubble is a complete sphere (equation 1); the other is the adhesion force (F_a) from the catalyst film underlying, which can be expressed as equation 2. The gravity of the gas bubble is neglected because of the much smaller density of gas relative to that of the liquid. If the gas bubble is going to be detached from the surface, the buoyant force should become large enough to match with the adhesion force (equation 3). Therefore, theoretically, the releasing diameter of the gas bubble is dependent from the adhesion force from the catalyst film. Derived from the equations 1-3, the radius of the gas bubble is proportional to the product of the root of γ and sine function of α (equation 4).

$$F_b = \rho \cdot g \cdot \frac{4}{3} \pi \cdot r^3 \quad \text{Eq. 1}$$

$$F_a = \gamma \cdot 2\pi(r \cdot \sin\alpha) \cdot \sin\alpha \quad \text{Eq. 2}$$

$$F_b = F_a \quad \text{Eq. 3}$$

$$r \propto \sqrt{\gamma} \cdot \sin\alpha \quad \text{Eq. 4}$$

Where ρ is the density of the electrolyte, g is the gravitational acceleration, r is the radius of the gas bubble, γ is the surface tension of the catalyst film and α is the angle between horizontal direction and the tangent direction of the contact point of gas bubble and catalyst film.

The adhesion force originates from the triple phase (solid-liquid-gas) contact line (TPCL), which is a continuous circle for an absolutely flat film (Figure 1B, left). Constructing nanostructured film can offer a much rougher surface, which significantly decreases the surface solid fraction and thus cuts the TPCL into discontinuous dots (Figure 1B, right). Given that each point of the TPCL possesses the same adhesion force to the gas bubble for the same material, the broken TPCL would show a much smaller accumulated adhesion force relative to the continuous TPCL. Moreover, direct growth of the nanostructures can bring about many other advantages, such as good electron transportation and high porosity, which make the catalyst film more conductive and facilitate the penetration of electrolyte (reactant), leading to the improvement of catalytic performance.

3. Realization and demonstration of low-adhesion electrodes

3.1 Hydrogen evolution reaction (HER)

HER is a typical example of GERs, as it has a variety of applications for energy conversion processes.^{23, 24} This reaction needs catalysts to reduce the overpotential to operate this reaction,

and the activities of the catalysts are highly dependent on their electronic structures.²⁵⁻²⁷ About a decade ago, MoS₂ was emerged as an efficient catalyst for HER due to the suitable binding energy to hydrogen (not too strong or not too weak) at the edge sites, thus the Mo edges are considered as active sites for MoS₂.^{13, 28-33} Recently, many compounds have been synthesized and identified with superior HER activities because of the new active sites, such as WS₂³⁴, CoSe₂²³, CoS₂^{35, 36}, NiP³⁷, CoP^{38, 39}, Mo₂C⁴⁰, MoB⁴¹ and so on. More recently, metal free catalysts are also investigated with high HER performance.^{42, 43} To further optimize their HER performance, rational design of the structures of the catalysts are now being actively pursued.⁴⁴

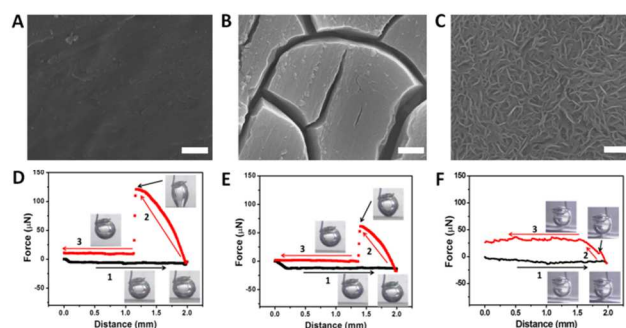


Figure 2. (A), (B) and (C), the different surface morphologies of MoS₂ films; (D), (E) and (F), the corresponding gas bubble adhesion forces of the above surface structures. (Reprinted with permission from Ref. [20], Copyright 2014, Wiley-VCH)

Our group has employed MoS₂ as the electro-catalyst to demonstrate the effectiveness of the low-adhesion surface according to the structural designing.²⁰ Three MoS₂ films with different surface architectures (nanostructured, microstructured and flat films) were fabricated by *in-situ* sulfidation and precipitation processes, as shown in Figure 2A, B and C. The adhesion force measurements revealed that the flat film exhibited a strong interaction to the gas bubble while the nanostructured film showed a negligible response (Figure 2D-F), indicating that constructing nanoporous surface was an efficient approach to reduce the adhesion force towards gas bubbles. In addition, the contact angle of a gas bubble on the nanostructured surface is larger than 150°, thus making the surface with low adhesion force (equation 2) and “superaerophobic”.

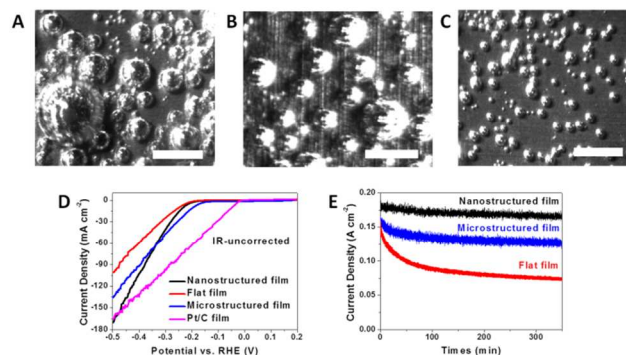


Figure 3. (A), (B) and (C), different gas evolution behaviors on the flat, microstructured and nanostructured MoS₂ films; (D), HER performances of the 3 MoS₂ films and commercial 20 wt%

Pt/C film fabricated by drop-casting method; (E), stability results of the 3 MoS₂ films. (Reprinted with permission from Ref. [20], Copyright 2014, Wiley-VCH)

The difference on the releasing sizes of the as-formed hydrogen bubbles is the consequence of constructing different surface architectures. As shown in Figure 3A-C, the flat film that possesses the highest adhesion force shows the biggest releasing size of the gas product (~500 μm in diameter), while the microstructured film can reduce the diameter to ~300 μm. It is found that the releasing size of gas bubbles on nanostructured surface is as small as 50-100 μm, demonstrating the effectiveness of nano-engineering for reducing the solid-gas interaction. The reduced gas bubble size would give rise to the in-time leaving of the adhered gas bubbles and thus diminishes the negative effects (blocking electrolyte penetration and covering working area). As a result, the nanostructured film shows the fastest hydrogen evolution current density increase and the most stable working state (Figure 3D and E). Specifically, for the flat and the nanostructured films, their electrochemical surface areas (can be correlated to the active sites density), Tafel slopes, exchange current densities and series resistances are very close, thus the different current density increase can only be correlated to the different bubble evolution behaviors.

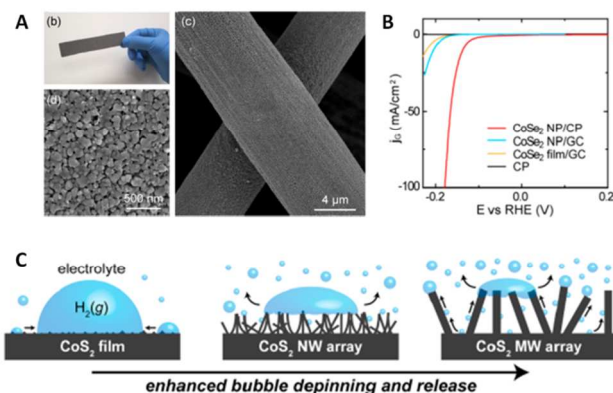


Figure 4. (A) and (B), surface characterizations and HER performance of CoSe₂ nanostructured film, (Reprinted with permission from Ref. [33], Copyright 2014, ACS); (C), schematic illustration of the evolution behavior of as-formed gas bubbles on CoS₂ films with different surface structures. (Reprinted with permission from Ref. [35], Copyright 2014, ACS)

This effect can also be expanded successfully to other electrocatalysts for HER. Kong et al. have firstly identified a highly-efficient catalyst of CoSe₂ with comparable performance to Pt²³, and further they developed a method to grow a CoSe₂ nanoparticulate film (Figure 4A) on a curved substrate to form a three-dimensional electrode, which could deliver a high HER current density at low overpotential and a stable state over a long period (Figure 4B)⁴⁵. Faber et al. also demonstrated the enhanced bubble-releasing effect by constructing three different metallic CoS₂ films (flat, microwire and nanowire film) and comparing their HER performances (Figure 4C).³⁵

3.2 Oxygen evolution reaction (OER)

Besides HER, OER is another important component of overall water splitting reaction. Since four electrons are involved to form one molecular of oxygen, this reaction possesses a more sluggish kinetic relative to the HER, thus more efficient catalysts are required to overcome the high reaction barrier.⁴⁶ Noble metal oxides (IrO₂ and RuO₂) are the best catalysts for water oxidation, but their scarcities greatly restricted their large-scale application.⁴⁷ Alternatively, since nickel and cobalt are identified to be the active center for OER, nickel and cobalt based materials (e.g. mixed transition metal oxides/hydroxides⁴⁸⁻⁵⁹, cobalt-based perovskites^{60,61} and cobalt phosphates^{62,63}) are demonstrated with comparable OER activities. Recently, carbon based metal free catalysts are also investigated with high OER activity.^{64, 65} Similarly, building oriented nanostructures is an effective approach to further improve the overall performance.

Li et al. found that incorporating nickel into cobalt oxides nanowire arrays could increase the surface roughness and thereby enhance the OER performance⁶⁶, which is also observed by Lu et al.⁶⁷. Our group also demonstrated that combining the intrinsically active electro-catalysts (NiFe-LDHs and Zn-doped cobalt oxides) with appropriate morphologies (nanoarrays⁶⁸ and hierarchical nanoarrays⁶⁹) would readily achieve high OER current densities with low overpotentials. This ultrahigh performance was also partially attributed to the low adhesion force of the electrodes to gas products, as demonstrated in the study of hierarchical NiCoFe-LDH nanoarrays⁷⁰. Although the hierarchical nanoarrays did not show a great improvement for further reducing the adhesion force compared with the nanoarrays, the higher porosity and active sites density endowed the electrode with a marginal enhancement for the overall performance. The aforementioned works indicate the performance of OER electrodes can also be benefited by constructing nanoarrays or hierarchical nanoarrays.

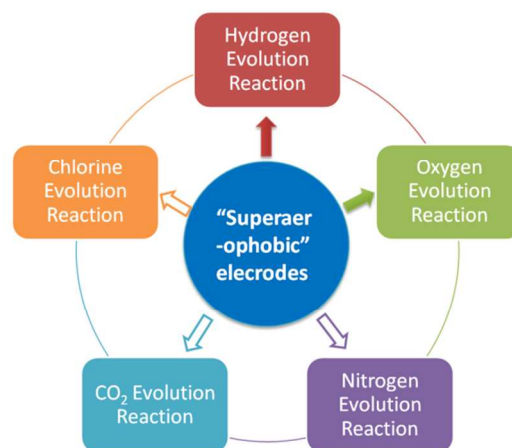


Figure 5. The usages of the low adhesion electrodes. The usages directed by solid arrows have been demonstrated and the usages directed by hollow arrows need to be further explored.

4. Summary and outlook

In this review, several recent works on engineering surface structures of electro-catalysts for GERs are summarized. Besides the high porosity and enhanced conductivity, the nanoarrays and hierarchical nanoarrays can effectively alleviate the adhesion to the gas bubbles, thus affording a fast gas releasing behavior,

resulting in a fast current increase and stable working state. This effect has been successfully applied in several non-noble electrocatalysts for both HER and OER, demonstrating the general efficacy of this concept.

Accordingly, as the noble metal catalysts (Pt, IrO₂ and RuO₂) show the highest intrinsic activities to the corresponding GERs, it is highly expected that ultrahigh performances would be achieved if these catalysts are built into oriented nanoarrays or hierarchical nanoarrays. In addition, since the catalysis reactions only occur at the surface, the noble catalysts can be deposited on the as-prepared conductive nanoarrays or hierarchical nanoarrays to reduce the amount of noble elements without the compromise of the catalytic performances.

Besides HER and OER, this approach should also be valid for other GERs (e.g. methanol oxidation, hydrazine oxidation and chlorine evolution reactions, figure 5) which are essential in national economy but suffer from severe adhesion of the gas products (CO₂, N₂ and Cl₂). It is well known that methanol oxidation and hydrazine oxidation both are important anodic reactions in direct liquid fuel cells and also suffer from severe bubble adhesion problem.^{71, 72} Therefore, in the near future, progresses on engineering the catalyst materials for these reactions should be required to circumvent the bubble adhesion problem and substantially improve the GERs performances.

Acknowledgments

This work was financially supported by the National Natural Science Foundation of China, the 973 Program (2011CBA00503 and 2011CB932403), the Program for New Century Excellent Talents in Universities, and the Program for Changjiang Scholars and Innovative Research Team in University.

Notes and references

^a State Key Laboratory of Chemical Resource Engineering, Beijing University of Chemical Technology, Beijing 100029, China
Tel.: +86-10-64448751. Fax: +86-10-64425385.
E-mail: sunxm@mail.buct.edu.cn

† These two authors contribute equally to this work.

1. T. R. Cook, D. K. Dogutan, S. Y. Reece, Y. Surendranath, T. S. Teets and D. G. Nocera, *Chem. Rev.*, 2010, 110, 6474-6502.
2. M. G. Walter, E. L. Warren, J. R. McKone, S. W. Boettcher, Q. Mi, E. A. Santori and N. S. Lewis, *Chem. Rev.*, 2010, 110, 6446-6473.
3. Y. Li and H. Dai, *Chem. Soc. Rev.*, 2014, 43, 5257-5275.
4. J.-M. Tarascon and M. Armand, *Nature*, 2001, 414, 359-367.
5. I. Moussallem, J. Jörissen, U. Kunz, S. Pinnow and T. Turek, *J. Appl. Electrochem.*, 2008, 38, 1177-1194.
6. P. Argyropoulos, K. Scott and W. Taama, *Electrochim. Acta*, 1999, 44, 3575-3584.
7. H. Yang, T. Zhao and Q. Ye, *J. Power Sources*, 2005, 139, 79-90.
8. W. Qian, D. P. Wilkinson, J. Shen, H. Wang and J. Zhang, *J. Power Sources*, 2006, 154, 202-213.
9. D. K. Bediako, B. Lassalle-Kaiser, Y. Surendranath, J. Yano, V. K. Yachandra and D. G. Nocera, *J. Am. Chem. Soc.*, 2012, 134, 6801-6809.
10. P. Du, O. Kokhan, K. W. Chapman, P. J. Chupas and D. M. Tiede, *J. Am. Chem. Soc.*, 2012, 134, 11096-11099.
11. M. W. Kanan, J. Yano, Y. Surendranath, M. Dinca, V. K. Yachandra and D. G. Nocera, *J. Am. Chem. Soc.*, 2010, 132, 13692-13701.
12. M. A. Lukowski, A. S. Daniel, F. Meng, A. Forticaux, L. Li and S. Jin, *J. Am. Chem. Soc.*, 2013, 135, 10274-10277.
13. B. Hinnemann, P. G. Moses, J. Bonde, K. P. Jørgensen, J. H. Nielsen, S. Hørch, I. Chorkendorff and J. K. Nørskov, *J. Am. Chem. Soc.*, 2005, 127, 5308-5309.
14. H. Wang, Z. Lu, S. Xu, D. Kong, J. J. Cha, G. Zheng, P.-C. Hsu, K. Yan, D. Bradshaw and F. B. Prinz, *Proc. Natl. Acad. Sci. USA*, 2013, 110, 19701-19706.
15. Y. Liang, Y. Li, H. Wang and H. Dai, *J. Am. Chem. Soc.*, 2013, 135, 2013-2036.
16. J. Xie, J. Zhang, S. Li, F. Grote, X. Zhang, H. Zhang, R. Wang, Y. Lei, B. Pan and Y. Xie, *J. Am. Chem. Soc.*, 2013, 135, 17881-17888.
17. H. Wang, Z. Lu, D. Kong, J. Sun, T. M. Hymel and Y. Cui, *ACS nano*, 2014, 8, 4940-4947.
18. Y. H. Chang, C. T. Lin, T. Y. Chen, C. L. Hsu, Y. H. Lee, W. Zhang, K. H. Wei and L. J. Li, *Adv. Mater.*, 2013, 25, 756-760.
19. J. Wang, H. x. Zhong, Y. l. Qin and X. b. Zhang, *Angew. Chem. Int. Ed.*, 2013, 125, 5356-5361.
20. Z. Lu, W. Zhu, X. Yu, H. Zhang, Y. Li, X. Sun, X. Wang, H. Wang, J. Wang and J. Luo, *Adv. Mater.*, 2014, 26, 2683-2687.
21. M. Wang, Z. Wang and Z. Guo, *Int. J. Hydrogen Energ.*, 2010, 35, 3198-3205.
22. S.-D. Li, C.-C. Wang and C.-Y. Chen, *Electrochim. Acta*, 2009, 54, 3877-3883.
23. D. Kong, J. J. Cha, H. Wang, H. R. Lee and Y. Cui, *Energy Environ. Sci.*, 2013, 6, 3553-3558.
24. M. Gong, W. Zhou, M.-C. Tsai, J. Zhou, M. Guan, M.-C. Lin, B. Zhang, Y. Hu, D.-Y. Wang and J. Yang, *Nat. Commun.*, 2014, 5.
25. D. Voiry, H. Yamaguchi, J. Li, R. Silva, D. C. Alves, T. Fujita, M. Chen, T. Asefa, V. B. Shenoy and G. Eda, *Nat. Mater.*, 2013, 12, 850-855.
26. J. Xie, H. Zhang, S. Li, R. Wang, X. Sun, M. Zhou, J. Zhou, X. W. D. Lou and Y. Xie, *Adv. Mater.*, 2013, 25, 5807-5813.
27. D. Merki, H. Vrubel, L. Rovelli, S. Fierro and X. Hu, *Chem. Sci.*, 2012, 3, 2515-2525.
28. H. I. Karunadasa, E. Montalvo, Y. Sun, M. Majda, J. R. Long and C. J. Chang, *Science*, 2012, 335, 698-702.
29. T. F. Jaramillo, K. P. Jørgensen, J. Bonde, J. H. Nielsen, S. Hørch and I. Chorkendorff, *Science*, 2007, 317, 100-102.
30. T. Wang, J. Zhuo, K. Du, B. Chen, Z. Zhu, Y. Shao and M. Li, *Adv. Mater.*, 2014, 26, 3761-3766.
31. D. Merki and X. Hu, *Energy Environ. Sci.*, 2011, 4, 3878-3888.
32. T. Wang, L. Liu, Z. Zhu, P. Papakonstantinou, J. Hu, H. Liu and M. Li, *Energy Environ. Sci.*, 2013, 6, 625-633.
33. D. Kong, H. Wang, J. J. Cha, M. Pasta, K. J. Koski, J. Yao and Y. Cui, *Nano Lett.*, 2013, 13, 1341-1347.
34. L. Cheng, W. Huang, Q. Gong, C. Liu, Z. Liu, Y. Li and H. Dai, *Angew. Chem. Int. Ed.*, 2014, 53, 7860-7863.

35. M. S. Faber, R. Dzedzic, M. A. Lukowski, N. S. Kaiser, Q. Ding and S. Jin, *J. Am. Chem. Soc.*, 2014, 136, 10053-10061.
36. Y. Sun, C. Liu, D. C. Grauer, J. Yano, J. R. Long, P. Yang and C. J. Chang, *J. Am. Chem. Soc.*, 2013, 135, 17699-17702.
37. E. J. Popczun, J. R. McKone, C. G. Read, A. J. Biacchi, A. M. Wiltrout, N. S. Lewis and R. E. Schaak, *J. Am. Chem. Soc.*, 2013, 135, 9267-9270.
38. Z. Pu, Q. Liu, P. Jiang, A. M. Asiri, A. Y. Obaid and X. Sun, *Chem. Mater.*, 2014, 26, 4326-4329.
39. J. Tian, Q. Liu, A. M. Asiri and X. Sun, *J. Am. Chem. Soc.*, 2014, 136, 7587-7590.
40. L. Liao, S. Wang, J. Xiao, X. Bian, Y. Zhang, M. D. Scanlon, X. Hu, Y. Tang, B. Liu and H. H. Girault, *Energy Environ. Sci.*, 2014, 7, 387-392.
41. H. Vrubel and X. Hu, *Angew. Chem. Int. Ed.*, 2012, 124, 12875-12878.
42. Y. Zhao, F. Zhao, X. Wang, C. Xu, Z. Zhang, G. Shi and L. Qu, *Angew. Chem. Int. Ed.*, 2014, 53, 13934-13939.
43. Y. Zheng, Y. Jiao, Y. Zhu, L. H. Li, Y. Han, Y. Chen, A. Du, M. Jaroniec and S. Z. Qiao, *Nat. Commun.*, 2014, 5, 3783-3790.
44. J. Kibsgaard, Z. Chen, B. N. Reinecke and T. F. Jaramillo, *Nat. Mater.*, 2012, 11, 963-969.
45. D. Kong, H. Wang, Z. Lu and Y. Cui, *J. Am. Chem. Soc.*, 2014, 136, 4897-4900.
46. I. C. Man, H.-Y. Su, F. Calle-Vallejo, H. A. Hansen, J. I. Martínez, N. G. Inoglu, J. Kitchin, T. F. Jaramillo, J. K. Nørskov and J. Rossmeisl, *ChemCatChem*, 2011, 3, 1159-1165.
47. A. Di Blasi, C. D'Urso, V. Baglio, V. Antonucci, R. Ornelas, F. Matteucci, G. Orozco, D. Beltran, Y. Meas and L. Arriaga, *J. Appl. Electrochem.*, 2009, 39, 191-196.
48. M. W. Louie and A. T. Bell, *J. Am. Chem. Soc.*, 2013, 135, 12329-12337.
49. L. Trotochaud, S. L. Young, J. K. Ranney and S. W. Boettcher, *J. Am. Chem. Soc.*, 2014, 136, 6744-6753.
50. M. Gong, Y. Li, H. Wang, Y. Liang, J. Z. Wu, J. Zhou, J. Wang, T. Regier, F. Wei and H. Dai, *J. Am. Chem. Soc.*, 2013, 135, 8452-8455.
51. T. Maiyalagan, K. A. Jarvis, S. Therese, P. J. Ferreira and A. Manthiram, *Nat. Commun.*, 2014, 5, 3949-3956.
52. Z. Lu, H. Wang, D. Kong, K. Yan, P.-C. Hsu, G. Zheng, H. Yao, Z. Liang, X. Sun and Y. Cui, *Nat. Commun.*, 2014, 5, 4345-4351.
53. R. D. Smith, M. S. Prévot, R. D. Fagan, Z. Zhang, P. A. Sedach, M. K. J. Siu, S. Trudel and C. P. Berlinguette, *Science*, 2013, 340, 60-63.
54. L. Trotochaud, J. K. Ranney, K. N. Williams and S. W. Boettcher, *J. Am. Chem. Soc.*, 2012, 134, 17253-17261.
55. R. D. Smith, M. S. Prévot, R. D. Fagan, S. Trudel and C. P. Berlinguette, *J. Am. Chem. Soc.*, 2013, 135, 11580-11586.
56. J. Landon, E. Demeter, N. İnoğlu, C. Keturakis, I. E. Wachs, R. Vasić, A. I. Frenkel and J. R. Kitchin, *ACS Catal.*, 2012, 2, 1793-1801.
57. T. Alexis, *Energy Environ. Sci.*, 2014, 7, 682-688.
58. J. B. Gerken, S. E. Shaner, R. C. Masse, N. J. Porubsky and S. Stahl, *Energy Environ. Sci.*, 2014, 7, 2376-2382.
59. Y. Xie, Y. Sun, S. Gao, F. Lei, J. Liu and L. Liang, *Chem. Sci.*, 2014, 5, 3976-3982.
60. J. Suntivich, K. J. May, H. A. Gasteiger, J. B. Goodenough and Y. Shao-Horn, *Science*, 2011, 334, 1383-1385.
61. A. Grimaud, K. J. May, C. E. Carlton, Y.-L. Lee, M. Risch, W. T. Hong, J. Zhou and Y. Shao-Horn, *Nat. Commun.*, 2013, 4, 2439-2445.
62. M. W. Kanan and D. G. Nocera, *Science*, 2008, 321, 1072-1075.
63. H. S. Ahn and T. D. Tilley, *Adv. Funct. Mater.*, 2013, 23, 227-233.
64. Y. Zhao, R. Nakamura, K. Kamiya, S. Nakanishi and K. Hashimoto, *Nat. Commun.*, 2013, 4, 2390-2396.
65. T. Y. Ma, S. Dai, M. Jaroniec and S. Z. Qiao, *Angew. Chem. Int. Ed.*, 2014, 53, 7281-7285.
66. Y. Li, P. Hasin and Y. Wu, *Adv. Mater.*, 2010, 22, 1926-1929.
67. B. Lu, D. Cao, P. Wang, G. Wang and Y. Gao, *Int. J. Hydrogen Energy*, 2011, 36, 72-78.
68. Z. Lu, W. Xu, W. Zhu, Q. Yang, X. Lei, J. Liu, Y. Li, X. Sun and X. Duan, *Chem. Commun.*, 2014, 50, 6479-6482.
69. X. Liu, Z. Chang, L. Luo, T. Xu, X. Lei, J. Liu and X. Sun, *Chem. Mater.*, 2014, 26, 1889-1895.
70. Q. Yang, T. Li, Z. Lu, X. Sun and J. Liu, *Nanoscale*, 2014, 6, 11789-11794.
71. P. Argyropoulos, K. Scott and W. M. Taama, *Electrochim. Acta*, 1999, 44, 3575-3584.
72. H. Yang, T. S. Zhao and Q. Ye, *J. Power Sources*, 2005, 139, 79-90.